Article published online: 2023-01-13

Comparison of MRI Findings among Osteofibrous Dysplasia, Fibrous Dysplasia, and NonOssifying Fibroma of the Long Bone

Hiroki Kato[1] Masaya Kawaguchi[1] Rena Miyase[1] Ken Iwashima[1] Akihito Nagano[2] Masayuki Matsuo[1]

[1] Department of Radiology, Gifu University, Gifu, Japan
[2] Department of Orthopedic Surgery, Gifu University, Gifu, Japan

Address for correspondence Hiroki Kato, MD, Department of Radiology, Gifu University, 1-1 Yanagido, Gifu 501-1194, Japan (e-mail: hkato@gifu-u.ac.jp).

Indian J Radiol Imaging 2023;33:150–156.

Abstract

Background The characteristics of magnetic resonance imaging (MRI) findings among osteofibrous dysplasia (OFD), fibrous dysplasia (FD), and nonossifying fibroma (NOF) have yet to be determined.

Aims This study determines the differences of MRI features among OFD, FD, and NOF of the long bone.

Patients and Methods This study included 39 patients including 10 OFD, 13 with FD, and 16 with NOF of the long bone. All patients underwent preoperative MRI and histological examination. We retrospectively reviewed the MRIs and compared the imaging findings among the three pathologies.

Results The maximum diameter was significantly different among OFD (47.0 ± 18.6 mm), FD (59.0 ± 35.0 mm), and NOF (33.3 ± 15.0 mm) ($p < 0.05$). Multiplicity (60%, $p < 0.01$), eccentric distribution (100%, $p < 0.05$), septation (70%, $p < 0.01$), homogeneous intensity on T2-weighted images (70%, $p < 0.01$), homogeneous contrast enhancement (63%, $p < 0.05$), and intense contrast enhancement (88%, $p < 0.01$) were significantly more frequent in OFD. Centric distribution (69%, $p < 0.01$), cyst formation (54%, $p < 0.01$), and fluid-fluid level formation (31%, $p < 0.01$) were significantly more frequent in FD. Eccentric distribution (100%, $p < 0.01$), heterogeneous on T2-weighted images (100%, $p < 0.01$), predominant hypointensity on T2-weighted images (44%, $p < 0.01$), and the presence of intralesional hypointensity on T2-weighted images (88%, $p < 0.01$) were significantly more frequent in NOF.

Conclusion MRI features could differentiate OFD, FD, and NOF of the long bone.

Keywords
- MRI
- osteofibrous dysplasia
- fibrous dysplasia
- nonossifying fibroma

Introduction

Osteofibrous dysplasia (OFD), previously referred to as ossifying fibroma of the long bones, is a benign fibro-osseous lesion involving the tibia in approximately 90% of cases. OFDs are usually diaphyseal, especially involving the middle and distal third of the shaft and typically involving the anterior cortex.[1] They are more frequent in males and typically occur

article published online
January 13, 2023

DOI https://doi.org/10.1055/s-0042-1760363.
ISSN 0971-3026.

Thieme Medical and Scientific Publishers Pvt. Ltd., A-12, 2nd Floor, Sector 2, Noida-201301 UP, India

during the first two decades of life. Even though OFDs gradually grow in the first decade of life, most undergo spontaneous regression after puberty.

Furthermore, fibrous dysplasia (FD) is classified as a benign fibro-osseous lesion characterized by the replacement of normal elements of the bone by a disorganized fibrous tissue. FDs commonly occur in the proximal femur, tibia, humerus, ribs, and craniofacial bones in a decreasing order of incidence. The location is diaphyseal, and the epicenter is centric or eccentric. The average age of patients affected with FD is typically 20 to 30 years, and the male-to-female ratio is 1:1.[1] They are usually classified into three forms: monostotic form, which denotes a single bone involvement; polyostotic form, which denotes a multiple bone involvement; and McCune Albright syndrome, which is polyostotic FD with endocrine and skin changes. The prognosis is excellent; however, malignant transformation rarely occurs.

Nonossifying fibroma (NOF), also referred to as fibrous cortical defects, is a cortically based benign bone lesion consisting mainly of fibrous tissue. NOFs commonly occur in the metaphysis of the long bones, particularly the tibia and femur. The average age of patients affected with NOF is typically less than 20 years, and the male-to-female ratio is 2:1.[1] These lesions are typically self-limiting, and spontaneous resolution at skeletal maturity is usually observed, especially in smaller NOFs.

Histopathologically, the differentiation between OFD and FD is difficult because of the common histological characteristics of variably shaped spicules of woven bone separated by a fibrovascular stroma. Radiologically, differentiating OFD from NOF is difficult because of the common radiological characteristics of well-circumscribed cortical osteolysis. Although detailed magnetic resonance imaging (MRI) findings of OFD,[2] FD,[3–6] and NOF[7] have already been described, to the best of our knowledge, no study has compared the MRI findings among OFD, FD, and NOF. Hence, this study assesses MRI characteristics that can be used to differentiate among OFD, FD, and NOF of the long bone.

Methods

Patients

The study was approved by the human research committee of our Institutional Review Board and complied with the guidelines of the Health Insurance Portability and Accountability Act. The requirement for informed consent was waived because of the retrospective nature of this study. Using the electronic medical chart system of our university hospital, we searched for patients with histopathologically confirmed OFD, FD, and NOF of the long bone who underwent preoperative MRI between January 2005 and August 2020. In total, 39 patients were enrolled in this study, including 10 patients with OFD (mean age, 11.3 years; age range, 3–21 years; five men and five women), 13 patients with FD (mean age, 26.3 years; age range, 9–51 years; six men and seven women), and 16 patients with NOF (mean age, 13.4 years; age range, 8–22 years; nine men and seven women). Among these patients, local pain was observed in 9 of 10 (90%) patients with OFD, 12 of 13 (92%) patients with FD, and 14 of 16 (87%) patients with NOF, whereas 10% of OFD cases, 8% of FD cases, and 13% of NOF cases were asymptomatic. The primary sites included the tibia ($n = 18$), femur ($n = 13$), fibula ($n = 4$), humerus ($n = 2$), and radius ($n = 2$). The patients' characteristics are summarized in ►**Table 1**.

Magnetic Resonance Imaging

All 39 patients were examined using a 1.5-T MRI system (Signa Excite TwinSpeed 1.5T [GE Healthcare; Milwaukee, Wisconsin, United States], Intera Achieva 1.5T Pulsar [Philips Medical Systems, Best, the Netherlands], or Inginea Prodiva 1.5T CS [Philips Medical Systems, Best, the Netherlands]). All MRIs were obtained at a section thickness of 3 to 5 mm with an intersection gap of 1 to 2 mm and a field of view ranging from 16 × 16 cm to 40 × 40 cm. Axial and sagittal or coronal T1-weighted spin-echo (repetition time [TR]/ echo time [TE], 316–750/8–15 ms), T2-weighted fast spin-echo (TR/ TE, 3,000–5,971/82–104 ms), and fat-suppressed T2-weighted fast spin-echo (TR/TE, 2,425–6,431/81–104 ms) images were obtained in all 39 patients. In 31 patients (8 OFD, 11 FD, and 12 NOF), axial and sagittal or coronal fat-suppressed gadolinium-enhanced T1-weighted (TR/TE, 417–767/8–16 ms) images were obtained after the intravenous injection of 0.1 mmol/kg of gadopentetate dimeglumine (Magnevist, Bayer HealthCare, Leverkusen, Germany) or gadobutrol (Gadavist, Bayer HealthCare, Leverkusen, Germany).

Imaging Assessment

Two radiologists with 21 and 7 years of post-training experience in musculoskeletal imaging, respectively, individually reviewed all MRIs. The reviewers were unaware of any clinical information or pathological diagnoses. Any disagreement between the two reviewers was resolved through discussion until the reviewers reached consensus.

First, the maximum diameters of the bone lesions were measured using axial and sagittal or coronal MRIs. On axial images, the percentages of the involved marrow areas occupied by bone lesions were qualitatively scored using a four-point scale: 1, small occupying rates (1–25%) of the lesion; 2, moderate (26–50%); 3, extensive (51–75%); and 4, diffuse (76–100%).

Next, cortical protrusion, bowing deformity, multiplicity, and distribution were assessed on the MRIs. The distribution was classified into eccentric or central on axial images. On T2-weighted images, septation, cyst formation, and fluid-fluid level formation were assessed. On fat-suppressed T2-weighted images, bone marrow edema and surrounding soft-tissue edema were assessed.

Subsequently, the signal intensity on MRIs was qualitatively assessed. On T1-weighted images, the intralesional homogeneity, predominant signal intensity, and presence of intralesional hyperintensity due to fatty marrow or hemorrhage were assessed. Isointensity on T1-weighted images was defined as the same signal intensity relative to the skeletal muscles. On T2-weighted images, the intralesional homogeneity, predominant signal intensity, and presence of

Table 1 Patient characteristics

Characteristics	OFD	FD	NOF
Number of patients	10	13	16
Age (year)			
Range	3–21	9–51	8–22
Mean	11.3	26.3	13.4
Gender			
Male	5	6	9
Female	5	7	7
Clinical symptoms			
Local pain	10	12	14
Asymptomatic	0	1	2
Primary sites			
Tibia	10	2	6
Femur	0	8	5
Fibula	0	1	3
Humerus	0	0	2
Radius	0	2	0

Abbreviations: FD, fibrous dysplasia; NOF, non-ossifying fibroma; OFD, osteofibrous dysplasia.

intralesional hypointensity and hypointense rim were assessed. Hypointensity on T2-weighted images was defined as the same signal intensity relative to the skeletal muscles.

Finally, the homogeneity and degree of contrast enhancement were qualitatively assessed on contrast-enhanced T1-weighted images. The degree of contrast enhancement was classified into intense or mild.

Statistical Analysis

All statistical analyses were performed using SPSS version 24.0 (IBM Corp.; Armonk, New York, United States). The Welch test and Tukey/Games–Howell post hoc test was used to compare the maximum diameter and medullary occupying score among the three pathologies. Chi-squared test was performed to compare the qualitative assessments (cortical protrusion, bowing deformity, multiplicity, distribution, septation, cyst formation, fluid-fluid level formation, bone marrow edema, surrounding soft-tissue edema, intralesional homogeneity, predominant signal intensity, intralesional hyperintensity on T1-weighted images, intralesional hypointensity and hypointense rim on T2-weighted images, and homogeneity and degree of contrast enhancement) among the three pathologies. When chi-squared test among the three groups was performed by SPSS, adjusted residual was calculated from residual analysis. If adjusted residual is 1.96 or greater (or, alternatively, less than −1.96), its associated probability is less than 0.05. Similarly, if adjusted residual is 2.58 or greater (or, alternatively, less than −2.58), its associated probability is less than 0.01. *p*-Values of less than 0.05 were considered to be statistically significant.

Results

►**Table 2** summarizes the quantitative measurements and qualitative assessments. The maximum diameter was significantly different among OFD (47.0 ± 18.6 mm), FD (59.0 ± 35.0 mm), and NOF (33.3 ± 15.0 mm) ($p < 0.05$). However, no significant differences were observed in the medullary occupying score among the three pathologies ($p = 0.070$).

Multiplicity ($p < 0.01$), distribution ($p < 0.01$), septation ($p < 0.01$), cyst formation ($p < 0.01$), and fluid–fluid level formation ($p < 0.05$) were significantly different among the three pathologies. Multiplicity (60%, $p < 0.01$), eccentric distribution (100%, $p < 0.05$), and septation (70%, $p < 0.01$) were significantly more frequent in OFD (►**Fig. 1**). Centric distribution (69%, $p < 0.01$), cyst formation (54%, $p < 0.01$), and fluid–fluid level formation (31%, $p < 0.01$)

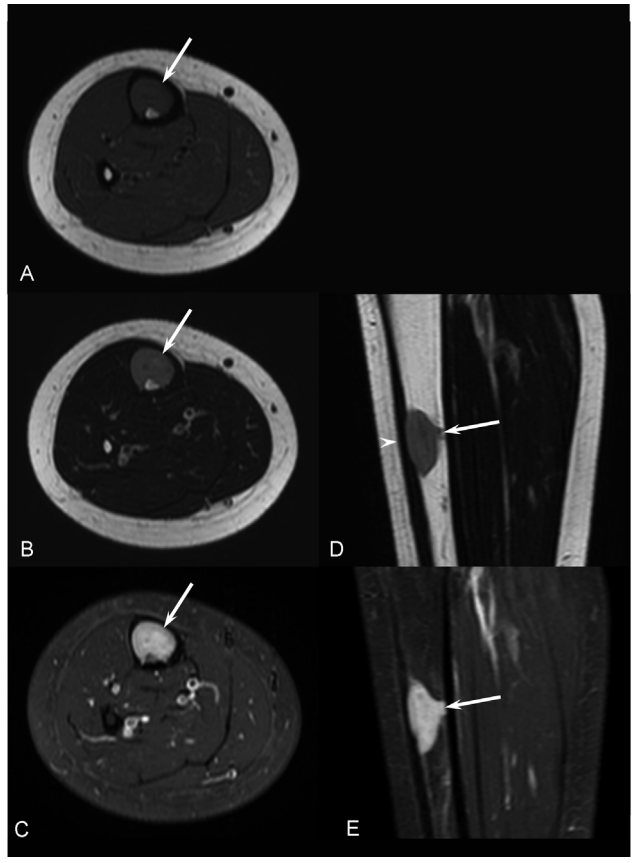

Fig. 1 A 5-year-old girl child patient with osteofibrous dysplasia of the right tibia. Magnetic resonance imagings show a well-demarcated, eccentric, homogeneous lesion appearing hypointense (arrow) on T1-weighted image (**A**), mildly hyperintense (arrows) on T2-weighted images (**B**/**D**) with cortical thinning (arrowhead), enhancing intensely (arrows) on fat-suppressed contrast-enhanced T1-weighted images (**C**/**E**).

Table 2 Quantitative measurements and qualitative assessments of OFD, FD, and NOF

Quantitative measurement	OFD	FD	NOF	*p*-Value
Maximum thickness (mm)	47.0 ± 18.6	59.0 ± 35.0	33.3 ± 15.0	0.034[a]
Medullary occupying score	3.0 ± 0.9	3.5 ± 0.9	2.5 ± 1.2	0.070
Qualitative assessment				
Cortical protrusion	7 (70)	9 (69)	10 (63)	0.899
Bowing deformity	3 (30)	6 (46)	3 (19)	0.282
Multiplicity	6 (60)[b]	1 (8)	0 (0)[c]	0.000[a]
Eccentric distribution	10 (100)[b]	4 (31)[c]	16 (100)	0.000[a]
Septation	7 (70)[b]	6 (46)	1 (6)[c]	0.003[a]
Cyst formation	0 (0)[c]	7 (54)[b]	2 (13)	0.004[a]
Fluid–fluid level formation	0 (0)	4 (31)[b]	0 (0)	0.012[a]
Bone marrow edema	2 (20)	3 (23)	6 (38)	0.553
Surrounding soft-tissue edema	2 (20)	3 (23)	5 (31)	0.788
Homogeneous intensity on T1WI	7 (70)	10 (77)	9 (56)	0.485
Predominant isointensity on T1WI	10 (100)	12 (92)	16 (100)	0.358
Hyperintensity on T1WI				
Fatty marrow	1 (10)	0 (0)	0 (0)	0.226
Hemorrhage	0 (0)	2 (15)	0 (0)	0.121
Homogeneous intensity on T2WI	7 (70)[b]	3 (23)	0 (0)[c]	0.000[a]
Predominant hypointensity on T2WI	0 (0)	0 (0)[c]	7 (44)[b]	0.002[a]
Hypointensity on T2WI	2 (20)[c]	5 (38)	14 (88)[b]	0.001[a]
Hypointense rim on T2WI	8 (80)	10 (77)	16 (100)	0.133
Homogeneous contrast enhancement	5 (63)[b]	3 (27)	1 (8)[c]	0.032[a]
Intense contrast enhancement	7 (88)[b]	3 (27)	4 (33)	0.019[a]

Abbreviations: FD, fibrous dysplasia; NOF, nonossifying fibroma; OFD, osteofibrous dysplasia; T1WI, T1-weighted images; T2WI, T2-weighted images.

Note: In quantitative measurement, data are presented as the mean ± 1 standard deviation. In qualitative assessment, data are numbers of patients, and numbers in parentheses are frequencies expressed as percentages. Isointensity on T1WI was defined as the same signal intensity relative to the muscles. Hypointensity on T2WI was defined as the same signal intensity relative to the muscles.

[a]Significant difference in value or frequency was found between OFD, FD, and NOF ($p < 0.05$).

[b]The frequencies were significantly higher than the others ($p < 0.05$).

[c]The frequencies were significantly lower than the others ($p < 0.05$).

were significantly more frequent in FD (►**Fig. 2**). Eccentric distribution (100%, $p < 0.01$) was significantly more frequent in NOF (►**Fig. 3**). However, no significant differences in cortical protrusion ($p = 0.899$), bowing deformity ($p = 0.282$), bone marrow edema ($p = 0.553$), and surrounding soft-tissue edema ($p = 0.788$) were observed among the three pathologies.

On T1-weighted images, no significant differences in the intralesional homogeneity ($p = 0.485$), predominant signal intensity ($p = 0.358$), intralesional hyperintensity due to fatty marrow ($p = 0.226$), and intralesional hyperintensity due to hemorrhage ($p = 0.121$) were observed among the aforementioned pathologies.

On T2-weighted images, intralesional homogeneity ($p < 0.01$), predominant signal intensity ($p < 0.01$), and the presence of hypointensity ($p < 0.01$) were significantly different among the three pathologies. Among the three pathologies, homogeneous intensity on T2-weighted images was most frequent in OFD (70%, $p < 0.01$), whereas it was least frequent in NOF (0%, $p < 0.01$). Moreover, among the aforementioned pathologies, predominant hypointensity on T2-weighted images was most frequent in NOF (44%, $p < 0.01$), whereas it was least frequent in FD (0%, $p < 0.05$). The presence of intralesional hypointensity on T2-weighted images was most frequent in NOF (88%, $p < 0.01$), whereas it was least frequent in OFD (20%, $p < 0.05$). However, no significant differences in the presence of hypointense rim on T2-weighted images ($p = 0.133$) were observed among the three pathologies.

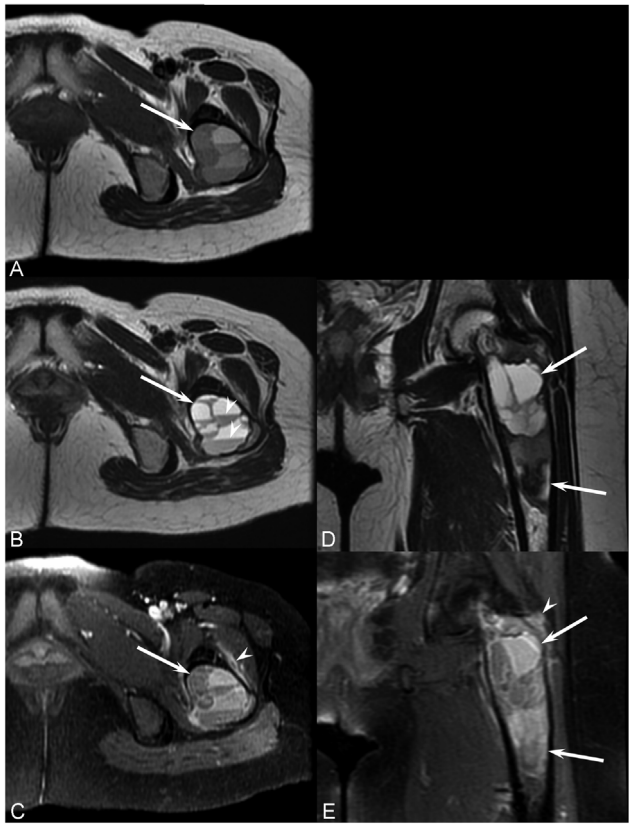

Fig. 2 A 27-year-old woman with fibrous dysplasia of the left femur. Magnetic resonance imagings show a multi-loculated, cystic, heterogeneous lesion appearing hyperintense (arrow) on T1-weighted image (**A**), hypo- to hyperintense (arrows) on T2-weighted images (**B**/**D**) with fluid-fluid level formations (arrowheads), enhancing mildly (arrows) on fat-suppressed contrast-enhanced T1-weighted images (**C**/**E**) with surrounding soft-tissue edema (arrowheads).

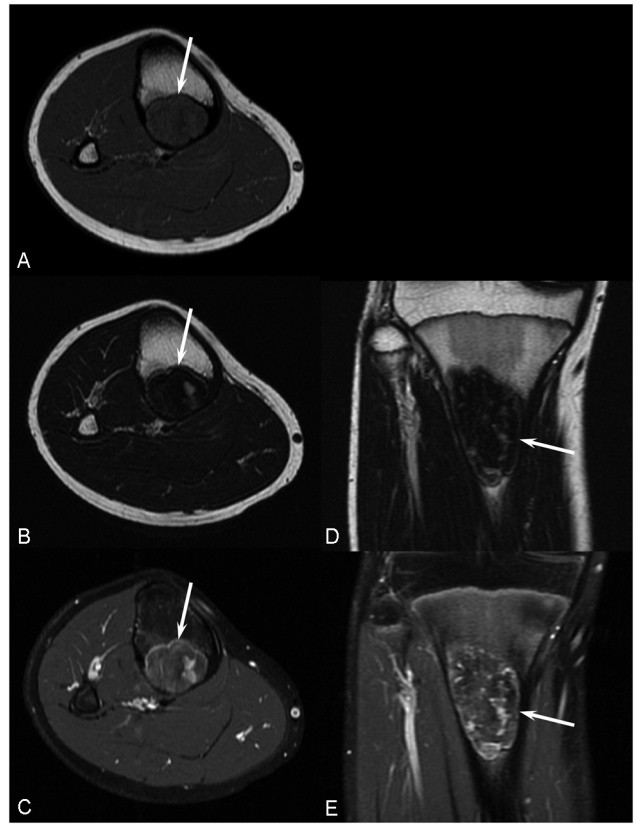

Fig. 3 A 12-year-old man with nonossifying fibroma of the right tibia. Magnetic resonance imagings show a well-demarcated, eccentric, homogeneous lesion appearing isointense (arrow) on T1-weighted image (**A**), predominantly hypointense (arrows) on T2-weighted images (**B**/**D**) with hypointense rim, enhancing mildly (arrows) on fat-suppressed contrast-enhanced T1-weighted images (**C**/**E**).

On contrast-enhanced T1-weighted images, homogeneity ($p < 0.05$) and degree ($p < 0.05$) of contrast enhancement were significantly different among the three pathologies. Among the three pathologies, homogeneous contrast enhancement was most frequent in OFD (63%, $p < 0.05$), whereas it was least frequent in NOF (8%, $p < 0.05$). Intense contrast enhancement was most frequent in OFD (88%, $p < 0.01$).

Discussion

OFD is typically an intracortical, well-marginated, lytic lesion with variable degrees of osteolysis and osteosclerosis and often with sclerotic margins.[8–10] OFD can present with a ground-glass appearance.[8] Scattered patchy sclerotic areas are often present within the lesion.[11] Osteolysis may present as a single focus, multiple bubble-like, or elongated linear foci interspersed with reactive bone.[10] In a study, OFD usually exhibited intermediate signal intensity on T1-weighted images and intermediate to high signal intensity on T2-weighted images.[2] They have reported that internal septa/multilocular appearance (92%) and cortical expansion (58%) were common MRI features of OFD, as with our results (septation, 70%; cortical protrusion, 70%).[2] However, the frequency of homogeneous signal intensity on T2-weighted images (70 vs. 17%) and homogeneous contrast enhancement on contrast-enhanced T1-weighted images (63 vs. 33%) are considerably different between the present and prior studies, respectively. In addition, they have reported that superimposed hemorrhagic or cystic, myxoid change, and even cartilaginous differentiation could modify the signal intensity and contribute to heterogeneous signal intensity on T2-weighted images.[2] However, according to a histopathological study, secondary changes such as hyalinization, hemorrhage, xanthomatous reaction, and cystic change were observed in only two of 20 (10%) OFD cases.[12] Because pathological secondary changes are rare in OFD, MRI features of OFD must depend on the amount and degree of fibroblast-like spindle cells, fibrous stroma, and bone trabeculae (woven bone) if pathological fracture does not occur. Although we believe that OFD usually exhibits homogeneous signal intensity on T2-weighted images and homogeneous contrast enhancement on contrast-enhanced T1-weighted images, further investigation is needed. In addition, a study has

reported that all 24 (100%) OFD cases exhibited diffuse and intense enhancement on contrast-enhanced T1-weighted images, as with our results (intense contrast enhancement, 88%).[2]

The radiological features of FD can be classified into three primary bony patterns: cystic, sclerotic, and mixed. FD typically appears as a radiolucent ground glass matrix, which is usually smooth and homogeneous, not centrally located within the medullary bone.[6] Although endosteal scalloping and cortical thinning may be present, a smooth outer cortical contour is always maintained. A thick layer of sclerotic bone is known as a rind sign.[6] The sclerotic margins can vary in thickness and may be interrupted or incomplete. MRI features of FD are usually nonspecific and variable and thus indicate that the diagnosis of FD cannot be based on MRI alone.[5] On T2-weighted sequences, FD displays variable signal intensities, consistent with the amount of degree of fibrous tissue, bone formation, and cystic or hemorrhagic changes.[3,13,14] Recently, a cloudy pattern on contrast-enhanced T1-weighted images has been reported as milk cloud appearance.[4] Hemorrhage and cystic change, either incipient or well-established, are characteristic pathological features of FD. Secondary changes including aneurysmal bone cyst-like change, form cells, or extensive myxoid change may occur. According to a histopathological study, secondary changes such as hyalinization, hemorrhage, xanthomatous reaction, and cystic change were observed in 22 of 62 (35%) FD cases.[12] Therefore, in this study, cyst formation (54%, $p < 0.01$) and fluid-fluid level formation (31%, $p < 0.01$) were significantly more frequent in FD.

NOF is typically an eccentric, well-delineated, multi or uniloculated, radiolucent lesion with sclerotic margins that are usually scalloped and slightly expansile.[7] The external outline of the cortical layer at the level of the lesion may be poorly visible or completely invisible.[15] MRI features of NOF depend on the relative amounts of hypercellular fibrous tissue, collagen, foamy histiocytes, hemorrhage, hemosiderin, and bone trabeculae.[7] Hypointense regions on T1- and T2-weighted images, which are characteristic MRI features of NOF and were observed in 15 of 19 (79%) NOF cases, have been correlated pathologically with hemosiderin and fibrous tissue elements.[7] Therefore, in this study, predominant hypointensity on T2-weighted images (44%, $p < 0.01$) and the presence of intralesional hypointensity on T2-weighted images (88%, $p < 0.01$) were significantly more frequent in NOF. In addition, because fibroblastic spindle cells with a storiform growth pattern, which exhibit relative hyperintensity on T2-weighted images, usually intervene in fibrous components, all 16 (100%) NOF cases in our series exhibited heterogeneous signal intensity on T2-weighted images.

This study had several limitations. First, this was a single-center retrospective analysis. Second, the cohort size was relatively small. Third, the management of OFD is usually consists of conservative measures, involving observation until the bone stops growing (skeletal maturity). The management of FD, including observation, conservative surgery, and radical surgical excision and reconstruction, depends on the age of the patient, growth rate, extent and location of the lesion, cosmetic deformity, and functional impairment. NOF is regarded as a "do not touch" lesion. Therefore, selection bias was definitely present because most of histologically proven cases included in this study were symptomatic and did not undergo surgery until they were symptomatic. Fourth, MRI findings were acquired with three different MRI scanners due to the retrospective nature of this study.

In conclusion, MRI findings, which depend on pathological findings, could contribute in differentiating OFD, FD, and NOF of the long bone. The MRI features of OFD were characterized by multiplicity, eccentric distribution, septation, homogeneous intensity on T2-weighted images, homogeneous contrast enhancement, and intense contrast enhancement. Moreover, the MRI features of FD were characterized by centric distribution, cyst formation, and fluid-fluid level formation. The MRI features of NOF were characterized by eccentric distribution, heterogeneous on T2-weighted images, predominant hypointensity on T2-weighted images, and presence of intralesional hypointensity on T2-weighted images.

References

1 Levine SM, Lambiase RE, Petchprapa CN. Cortical lesions of the tibia: characteristic appearances at conventional radiography. Radiographics 2003;23(01):157–177
2 Jung JY, Jee WH, Hong SH, et al. MR findings of the osteofibrous dysplasia. Korean J Radiol 2014;15(01):114–122
3 Jee WH, Choi KH, Choe BY, Park JM, Shinn KS. Fibrous dysplasia: MR imaging characteristics with radiopathologic correlation. Am J Roentgenol 1996;167(06):1523–1527
4 Franz D, Wechselberger J, Rasper M, et al. Milk cloud appearance-a characteristic sign of fibrous dysplasia on contrast-enhanced MR imaging. Eur Radiol 2019;29(07):3424–3430
5 Kinnunen AR, Sironen R, Sipola P. Magnetic resonance imaging characteristics in patients with histopathologically proven fibrous dysplasia-a systematic review. Skeletal Radiol 2020;49 (06):837–845
6 Kushchayeva YS, Kushchayev SV, Glushko TY, et al. Fibrous dysplasia for radiologists: beyond ground glass bone matrix. Insights Imaging 2018;9(06):1035–1056
7 Jee WH, Choe BY, Kang HS, et al. Nonossifying fibroma: characteristics at MR imaging with pathologic correlation. Radiology 1998; 209(01):197–202
8 Kahn LB. Adamantinoma, osteofibrous dysplasia and differentiated adamantinoma. Skeletal Radiol 2003;32(05):245–258
9 Khanna M, Delaney D, Tirabosco R, Saifuddin A. Osteofibrous dysplasia, osteofibrous dysplasia-like adamantinoma and adamantinoma: correlation of radiological imaging features with surgical histology and assessment of the use of radiology in contributing to needle biopsy diagnosis. Skeletal Radiol 2008; 37(12):1077–1084
10 Bethapudi S, Ritchie DA, Macduff E, Straiton J. Imaging in osteofibrous dysplasia, osteofibrous dysplasia-like adamantinoma, and classic adamantinoma. Clin Radiol 2014;69(02): 200–208
11 Castellote A, García-Peña P, Lucaya J, Lorenzo J. Osteofibrous dysplasia. A report of two cases. Skeletal Radiol 1988;17(07): 483–486

12 Sakamoto A, Oda Y, Iwamoto Y, Tsuneyoshi M. A comparative study of fibrous dysplasia and osteofibrous dysplasia with regard to expressions of c-fos and c-jun products and bone matrix proteins: a clinicopathologic review and immunohistochemical study of c-fos, c-jun, type I collagen, osteonectin, osteopontin, and osteocalcin. Hum Pathol 1999;30(12):1418–1426
13 Fisher AJ, Totty WG, Kyriakos M. MR appearance of cystic fibrous dysplasia. J Comput Assist Tomogr 1994;18(02):315–318
14 Fitzpatrick KA, Taljanovic MS, Speer DP, et al. Imaging findings of fibrous dysplasia with histopathologic and intraoperative correlation. Am J Roentgenol 2004;182(06):1389–1398
15 Błaż M, Palczewski P, Swiątkowski J, Gołębiowski M. Cortical fibrous defects and non-ossifying fibromas in children and young adults: the analysis of radiological features in 28 cases and a review of literature. Pol J Radiol 2011;76(04):32–39

